CanCNSM
Victoria
June 16-20, 1999

ANALYSIS OF INCOMPATIBLE MODES CONTRIBUTION IN LARGE STRAIN PLASTICITY AND LOCALISATION PROBLEMS

Felipe Gabaldón

Technical University of Madrid
School of Civil Engineering
28040 Zona Universitaria, MADRID, Spain
e-mail:felipe@filemon.mecanica.upm.es

Jose María Goicolea

Technical University of Madrid
School of Civil Engineering
28040 Zona Universitaria, MADRID, Spain
e-mail:goicolea@filemon.mecanica.upm.es

Carlos García-Garino

LAPIC, ITU, National University of Cuyo & CONICET
Casilla de Correo 947, 5500 Mendoza, Argentina
e-mail:cgarcia@pascal.uncu.edu.ar

Key Words: Enhanced Assumed Strain Elements, Incompatible Modes, Localisation, Large Strain Plasticity

Abstract. *This paper discusses the contribution of incompatible modes in the Enhanced Assumed Strain elements (EAS) in the context of large strain elastoplasticity and localisation problems. The key ideas of EAS formulation, the large strain constitutive model as well as the localisation criteria are briefly discussed. The first example studied is the extension of a plane strain element in order to discuss the instability that this kind of elements show when a standard Gauss integration rule (four points) is used. The following example analyze the behaviour of enhanced elements in comparison with Standard displacement elements (Q1) and mixed elements (Q1/P0) in order to capture localisation bands. In this case a single element test is performed computing numerically the acoustic tensor determinant. Finally the behaviour of the enhanced elements is discussed for the case of the stretch of a plane strain specimen when localisation bands appear.*

1 ASSUMED STRAIN ELEMENTS

The basis of enhanced assumed strain finite element formulation is the approximated solution of variational equations derived from Hu-Washizu functional. For the large strain problem the basic fields are displacements, stress tensor and deformation gradient tensor. The basic idea is to write the deformation gradient tensor $\boldsymbol{F}$ as an additive decomposition as follows:

$$\boldsymbol{F} = \underbrace{\boldsymbol{\nabla}_X \boldsymbol{\varphi}}_{\text{compatible}} + \underbrace{\tilde{\boldsymbol{F}}}_{\text{enhanced}} \tag{1}$$

where $\boldsymbol{\nabla}_X$ denotes gradient operator and $\boldsymbol{\varphi}$ is the *deformation* mapping that transforms the original (undeformed) configuration into the current (deformed) one. In this work the Q1/E4, Q1/ES4 and Q1/ET4 elements proposed by Simo, Armero and coworkers[1,7] have been used.

2 CONSTITUTIVE MODEL

The large strain elastoplastic constitutive model used is based on the multiplicative decomposition of deformation gradient[3] :

$$\boldsymbol{F} = \boldsymbol{F}^e \boldsymbol{F}^p \tag{2}$$

The numerical implementation is based on the multiplicative update of the elastic Finger tensor $\boldsymbol{b^{-1}} = \boldsymbol{F}^{-\mathrm{T}} \boldsymbol{F}^{-1}$, as proposed by García-Garino.[2] The corresponding numerical scheme is very easy to code and has rather low computational cost. The numerical scheme,[2] originally written in terms of *spatial* variables, has been recast in terms of *material* quantities in order to deal with the kinematics of enhanced elements. A predictor-corrector scheme is used in order to integrate the constitutive law:

- Elastic predictor: for given load step at time t, and the problem's data base: Ω_t, elastic Finger tensor $\boldsymbol{b}_t^{e^{-1}}$ and deformation gradient tensor $\boldsymbol{F}_t$; for a displacement increment $\Delta \boldsymbol{u}$ the trial intermediate configuration $\Omega_{t+\Delta t}^{\mathrm{PR}}$ is computed:

$$\left(\boldsymbol{F}_{t+\Delta t}^e\right)^{\mathrm{PR}} = \boldsymbol{F}_{t+\Delta t} \boldsymbol{F}_t^{p^{-1}} = \boldsymbol{f}_{\Delta t} \boldsymbol{F}_t^e \tag{3}$$

  where $\boldsymbol{f}_{\Delta t} = \boldsymbol{F}_{t+\Delta t} \boldsymbol{F}_t^{-1}$. Taking into account eq. (2), (3) and the Finger tensor definition a trial elastic Finger tensor is computed as:

$$\left(\boldsymbol{b}_{t+\Delta t}^{e^{-1}}\right)^{\mathrm{PR}} = \boldsymbol{f}_{\Delta t}^{-\mathrm{T}} \boldsymbol{b}_t^{e^{-1}} \boldsymbol{f}_{\Delta t}^{-1} \tag{4}$$

- Plastic Corrector: the flow rule is defined in the material configuration:[9]

$$\dot{\boldsymbol{C}}^p = 2\dot{\gamma} \boldsymbol{N} \tag{5}$$

where $\boldsymbol{C}^p = (\boldsymbol{F}^p)^{\mathrm{T}}\boldsymbol{F}$ is the plastic component of right Cauchy tensor and $\boldsymbol{N}$ denotes the normal vector to the yield surface. The flow rule is integrated using a backward-euler scheme. The updated (*spatial*) elastic Finger tensor $\boldsymbol{b}^{e^{-1}}_{t+\Delta t}$ is computed performing a Push-Forward[5] operation to the updated plastic component of right Cauchy tensor (See[2] for a detailed derivation):

$$\boldsymbol{b}^{e^{-1}}_{t+\Delta t} = \boldsymbol{b}^{e^{\mathrm{PR}^{-1}}}_{t+\Delta t} + 2\gamma \boldsymbol{n}_{t+\Delta t} \tag{6}$$

where the plastic multiplier γ is computed by means of a radial return algorithm.[10]

This model has been applied for the case of Von Mises (J2) plasticity.

LOCALISATION CRITERIA

In this work localisation bands are supossed to be weak discontinuities: The following hypothesis account for the necessary conditions required in order a band S with normal $\boldsymbol{n}$ takes place:

1. The velocity field $\dot{\boldsymbol{u}}$ is smooth for all time t.
2. The strain tensor can be discontinuos between both faces of S.
3. When localisation takes place the stress state is the same at both sides of S.

From these hypotheses localisation condition results:

$$\boldsymbol{Q}(\boldsymbol{n}) \cdot \boldsymbol{g} = 0 \tag{7}$$

where:

- $\boldsymbol{g}$ denotes the polarization vector.
- $\boldsymbol{Q}(\boldsymbol{n}) = \boldsymbol{n} \cdot \boldsymbol{C}_{\mathrm{ep}} \cdot \boldsymbol{n}$ is the acoustic tensor.
- $\boldsymbol{C}_{\mathrm{ep}}$ is the elastoplastic tangent tensor.

There are solutions of equation (7) different to the trivial one if:

$$\det(\boldsymbol{Q}(\boldsymbol{n})) = 0 \tag{8}$$

This localisation condition has been solved exactly using a symbolic algebra package,[4] for plane strain. The material law is Von Mises plasticity with constant isotropic hardening

H. Taking into account the incompressibility of plastic flow, the stress tensor for simple extension test results:

$$\boldsymbol{\sigma} = \begin{pmatrix} 0 & 0 & 0 \\ 0 & Y & 0 \\ 0 & 0 & \frac{1}{2}Y \end{pmatrix} \tag{9}$$

and the tangent elastoplastic tensor is:

$$\boldsymbol{C}_{\text{ep}} = \begin{pmatrix} \frac{\lambda\,\mu + \lambda\,H + \mu^2 + 2\,\mu\,H}{\mu + H} & \frac{\lambda\,\mu + \lambda\,H + \mu^2}{\mu + H} & 0 \\ \frac{\lambda\,\mu + \lambda\,H + \mu^2}{\mu + H} & \frac{\lambda\,\mu + \lambda\,H + \mu^2 + 2\,\mu\,H}{\mu + H} & 0 \\ 0 & 0 & \mu \end{pmatrix} \tag{10}$$

The normal vector $\boldsymbol{n}$ to the band is written in term of its orientation θ as $\boldsymbol{n} = (\cos(\theta),\, \sin(\theta))$, consequently the components of the acoustic tensor are:

$$\begin{aligned} Q_{11} &= \frac{\lambda\,\mu\cos^2\theta + \lambda\,H\cos^2\theta + \cos^2\theta\,\mu\,H + \mu^2 + \mu\,H}{\mu + H} \\ Q_{12} &= \frac{\cos\theta\sin\theta\,(\lambda\,\mu + \lambda\,H + 2\,\mu^2 + \mu\,H)}{\mu + H} \\ Q_{22} &= \frac{\lambda(\mu + H)\sin^2\theta + \mu\,H\sin^2\theta + \mu\,(\mu + H)}{\mu + H} \end{aligned}$$

The localisation equation (8) written in terms of acoustic tensor components results in the localisation condition:

$$H_{\text{crit}} = -\frac{\mu\,(2\cos^2\theta - 1)^2\,(\mu + \lambda)}{\lambda + 2\,\mu} \tag{11}$$

Equation (11) relates the critical hardening modulus H_{crit} with the orientation θ of localisation bands.

3 SINGLE ELEMENT SIMPLE TENSION TEST

In this problem the influence of Gauss integration rule on stability of enhanced elements is studied. The EAS elements are underintegrated when a four point Gauss integration rule is used, consequently hourglass modes appear for high strain levels. For this reason higher order integration rules are necessary in order to circurvent the problem.[8] In this problem the evolution of internal energy is studied and the obtained results are compared with elements that provide the exact solution (Q4 y Q1/P0).

The biunit square element is considered. The element is streched as shown in figure 1, where $\lambda_2 = 3$. The constitutive model is Von Mises elastoplasticity with an isotropic

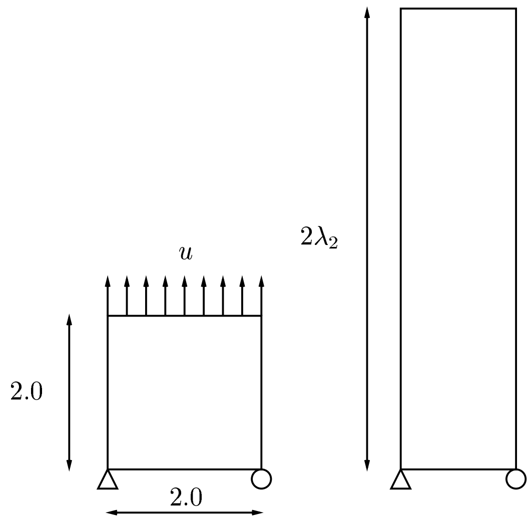

Figure 1: *Single element simple tension test*

hardening defined by a saturation law. The mechanical properties are: $E = 206.9$, $\nu = 0.29$, $\sigma_Y = 0.45 + 0.26\,(1 - e^{-16.93\varepsilon_p}) + 0.13\varepsilon_p$. Figure 2 show the deformed shapes obtained with four Gauss point integration rules. For a certain strech level the *hourglassing* phenomena appear, due to the fact that the element stiffness matrix is underintegrated. The enhanced modes are activated in a spurious way for Q1/E4, Q1/ES4 and Q1/ET4 elements, when the principal stretch λ_2 reach 1.52, 1.42 and 1.35 values respectively. This fact is clearly shown in figure 3 that plots the change of internal energy in terms of principal stretch λ_2. When a five or nine integration point rules are used the problem is aliviated but still in these cases a light hourglassing remains.

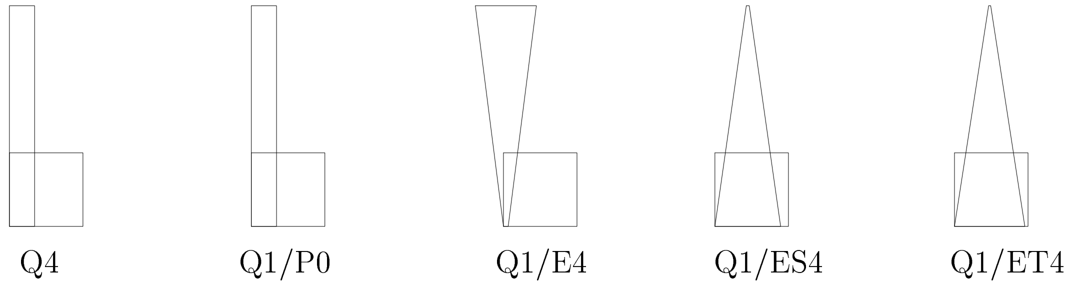

Figure 2: *Single element simple tension test. Deformed shapes for 4 Gauss point integration rule.*

4 SINGLE ELEMENT LOCALISATION TEST

In this problem, originally proposed for small strain case by Ortiz[6] and generalized later for large strain case,[11] the EAS elements behaviour is studied in order to capture localisation bands. In the figure 4 geometry and boundary conditions are shown. In the uppermost corner a horizontal displacement $u = 10$ is imposed. The material properties are $E =$

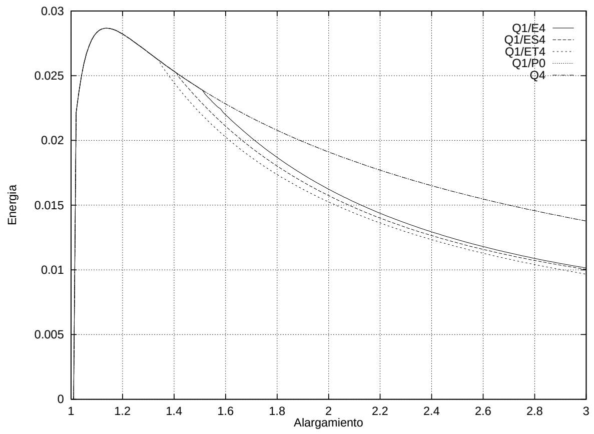

Figure 3: *Strain energy (incremental) for 4 Gauss point integration rule*

206.9, $\nu = 0.29$, $\sigma_y = 0.45$ and the saturation hardening law is the one proposed in.[7]

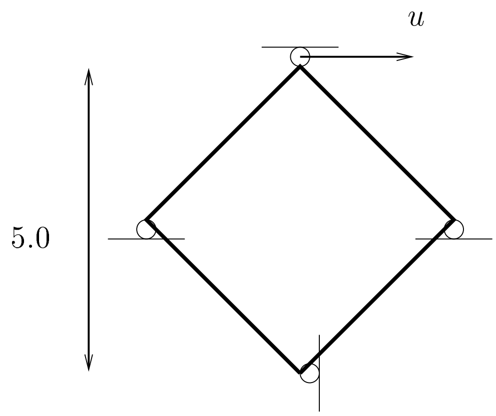

Figure 4: *Single element localisation test*

In figure 5 the deformed shapes for the different EAS elements integrated with five point rule, as well as the corresponding ones to standard elements Q1 y Q1/P0 are shown.

In order to study the performance of these elements for capturing localisation bands the determinant of acoustic tensor value is plotted along the whole load process. In a first phase it can be seen that the minimum values for $\det(\boldsymbol{Q})$ are found when the bands are oriented along the element diagonals. For these directions, in figure 6, the evolution of $\det(\boldsymbol{Q})$ in terms of displacement u is shown.

From the obtained results it can be concluded that when plastic flow takes place the determinant of acoustic tensor decreases for Q1 element and a minimum value is found for all the other ones. That minimum value is reached earlier for the enhanced elements. The same result is found for Q1/E4, Q1/ES4 and Q1/ET4 elements.

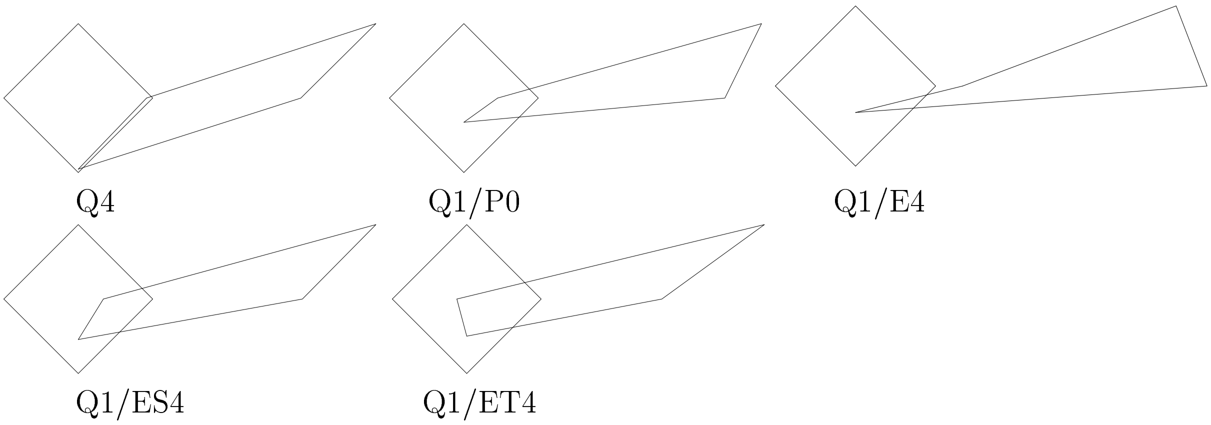

Figure 5: *Deformed shapes for EAS and standard elements*

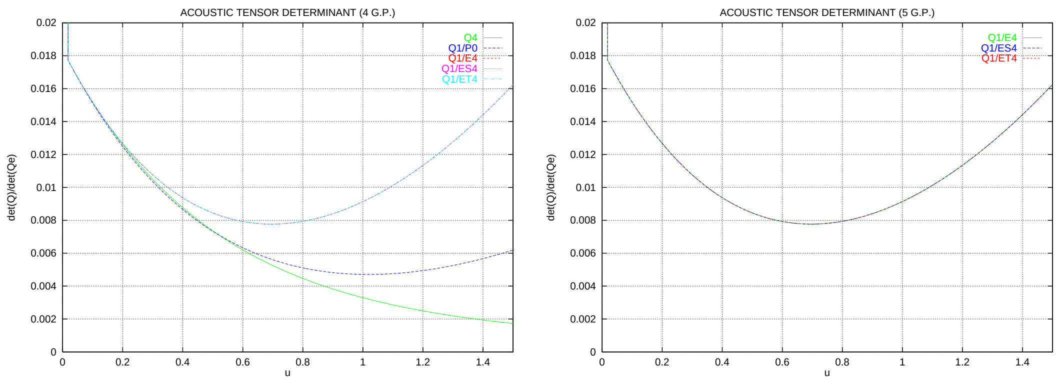

Figure 6: *Single element localisation test.to. Determinant of Acoustic tensor Evolution. Use of four and five gauss point integration rules.*

5 LOCALISATION IN THE SIMPLE TENSION TEST OF A PLANE STRAIN SPECIMEN

In this problem the onset of localisation bands is studied for a plane strain specimen under simple tension load. The definition of this example can be found in works of Simo et al.[7,8] The material hardening-softening law is a double parabola proposed by Ortiz.[6] In this work the results obtained for Q1/E4, Q1/ES4 y Q1/ET4 elements are compared. Different integration rules with 4, 5 and 9 integration points have been used. The Q1 and Q1/P0 elements have not been taken into account because are unable to capture localisation bands.

Figure 7 shows the localisation bands obtained for the different elements when a five point integration rule is used. As can be seen in this picture the bands are clearly captured for Q1/E4 and Q1/ES4 elements but are more difuse for the Q1/ET4 element. Figure 8 compares the captured bands when different gauss point integration rules are used for the Q1/E4 element. The bands are easily displayed for all rules used, but are more difuse as well as the quadrature order used in the integration rule increases because the element stiffness becomes higher.

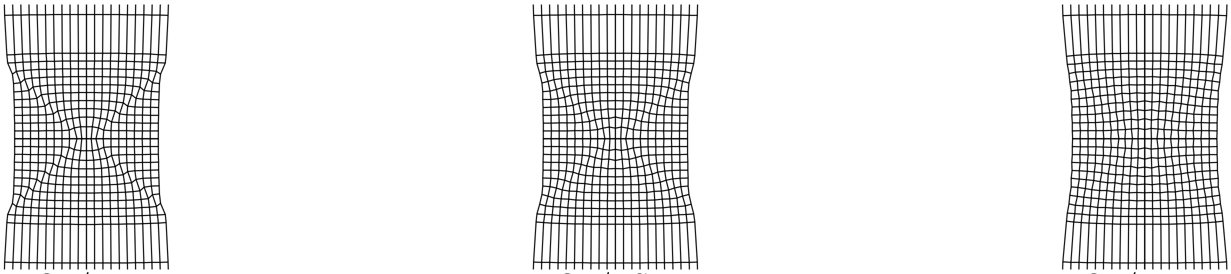

Q1/E4 Q1/ES4 Q1/ET4

Figure 7: *Localisation bands picture. Five gauss point integration rule*

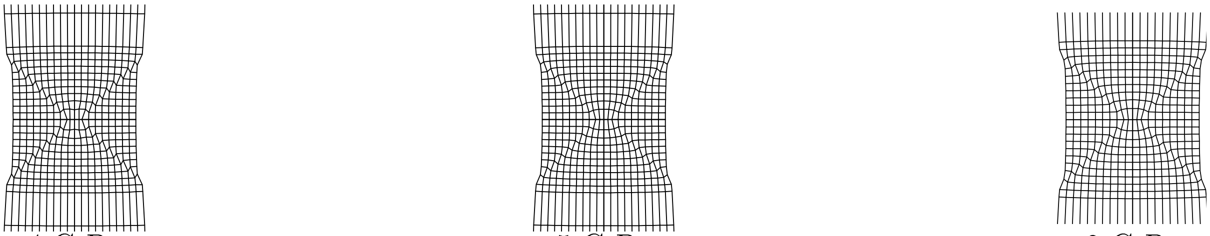

4 G.P. 5 G.P. 9 G.P.

Figure 8: *Localisation bands captured with Q1/E4 element*

The influence of the different quadrature orders and elements used on the obtained results is shown in figure 9 .

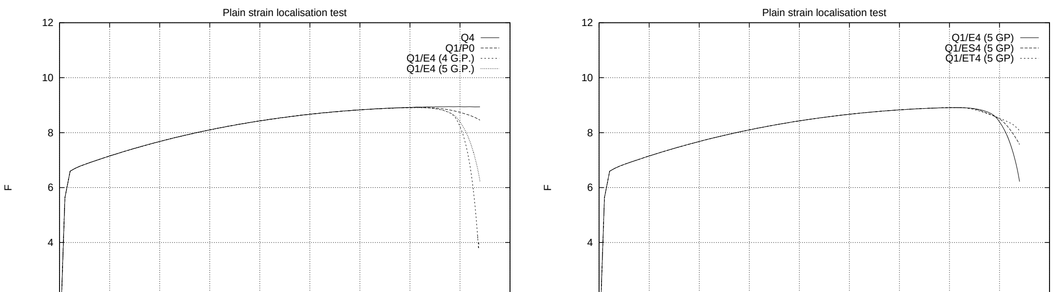

Figure 9: *Load-displacement curve: a) Results comparison of Q1, Q1/P0 and Q1/E4 elements for 4 and 5 point Gauss rule. b) Comparison of EAS results for 5 point Gauss rule.*

Figure 9a displays the different results obtained for Q1 standard element, Q1/P0 mixed element and the Q1/E4 enhanced element: these have been computed using both four and five point integration rules. In figure 9b the postpeak behaviour of different EAS elements is show when a five point integration rule is used.

6 CONCLUSIONS

The contribution of enhanced modes in the case of EAS elements is studied for large strain plasticity and localisation problems. The following methodology has been used:

- Analyse the internal energy evolution for some problems at the instant when numerical instability is prone to appear.
- Study the behaviour of the acoustic tensor determinant for localisation problems.

The obtained results allow to conclude:

1. Elements Q1/E4, Q1/ES4 and Q1/ET4 show similar instability behaviour.
2. Localisation bands are suitably captured by enhanced elements. The kinematics used for Q1/ET4 element leds to slighty more diffuse bands.
3. Higher order integration rules improve stability; however, they also increase slighty the element stiffness for postpeak behaviour.

7 ACKNOWLEGDMENTS

This work has been supported by Technical University of Madrid, in the framework of Latin Amrican activities, proyect AL98-0440-2.15 (Research and development of large strain and plasticity finite element models). The third author acknowledges the financial support granted by the Institute of Fundamental Sciences (Physics branch) at National University of Cuyo.

REFERENCES

[1] Armero F. and Glaser S. On the formulation of enhanced strain finite elements in finite deformations. Engieneering computations. Vol 14. pp 759-791. 1997.

[2] García Garino, C. A numerical model for the analysis of large strain elastoplastic solids. Ph.D. Thesis (in spanish). Polytechnic University of Catalonia. 1993.

[3] Lee, E.H., Elastic-Plastic deformation at finite strains, ASME Journal of Applied Mechanics, Vol. 36, pp. 1–6, 1969.

[4] MAPLE V. Library Reference Manual. Springer Verlag. 1993

[5] Marsden, J. y Hughes T.J.R. Mathematical Foundations of Elasticity. Dover. 1996

[6] Ortiz M., Leroy I. y Needleman A. A finite element method for localized failure analysis. Computer Methods in Applied Mechanics and Engineering. Vol 61, pp 189-214. 1988.

[7] Simo J.C. y Armero F. Geometrically nonlinear enhanced strain mixed methods and the method of incompatible modes. International Journal for Numerical Methods in Engineering. Vol 110. pp 359-386. 1993

[8] Simo J.C., Armero F. and Taylor R.L. Improved versions of assumed enhanced strain tri-linear elements for 3D finite deformation problems. Computer Methods in Applied Mechanics and Engineering. Vol 110. pp 359-386. 1993.

[9] Simo J.C. A framework for finite strain elastoplasticity based on maximum plastic dissipation and the multiplicative decomposition: parts I and II. Computer Methods in Applied Mechanics and Engineering. Vol 66. pp 199-219 and Vol 68. pp 1-31

[10] Simo J.C. Topics on the numerical analysis ans simulation of plasticity. Handbook of numerical analysis, Vol III. Ed. by P.G. Ciarlet and J.L. Lions. North Holland.

[11] Steinmann P. y Willam K. Finite elements for capturing localized failure. Arch. Appl. Mech. Vol 61, pp 259-275. 1990.